JAM CM Journal of Applied Mathematics and Computational Mechanics 2025, 24(2), 5-17
www.amcm.pcz.pl p-ISSN 2299-9965
DOI: 10.17512/jamcm.2025.2.01 e-ISSN 2353-0588

MODULATIONAL STABILITY OF WAVE PACKETS AT FLUID INTERFACE OF LAYER AND HALF-SPACE

Olga Avramenko[1], Volodymyr Naradovyi[2]

[1] *Department of Mathematics, National University of Kyiv Mohyla Academy*
Kyiv, Ukraine
[2] *Department of Informatics, Programming, Artificial Intelligence, and Technological Education*
Volodymyr Vynnychenko Central Ukraine State University
Kropyvnytskyi, Ukraine
o.avramenko@ukma.edu.ua, v.v.naradovyi@cuspu.edu.ua

Received: 6 November 2024; Accepted: 30 May 2025

Abstract. The modulational stability of internal wave packets propagated along the surface of a hydrodynamic system consisting of a lower half-space and an upper layer covered with a rigid lid is investigated. The study is conducted within the framework of a nonlinear low-dimensional model incorporating surface tension on an interface using the method of multi-scale expansions implemented via symbolic computation. The evolution equation of the envelope of the wave packet takes the form of the Schrödinger equation. Conditions for the modulational stability of the solution of the evolution equation are identified for various physical and geometrical characteristics of the system. Significant influence on the modulational stability of the system's geometrical characteristics and surface tension is observed for relatively small liquid layer thicknesses. For large layer thicknesses, the stability diagram degenerates to that of a system composed of two half-spaces.

MSC 2010: *76B55, 76E99*
Keywords: *modulational stability, internal waves, multi-scale expansions, surface tension, Benjamin-Feir index, evolution equation*

1. Introduction

This study examines wave packet propagation along the interface in a two-layer fluid system, accounting for surface tension. Research on nonlinear wave propagation in hydrodynamic systems, such as layers or half-spaces, has uncovered various instabilities, including modulational, or Benjamin-Feir, instability [1]. Zakharov [2] described the evolution of nonlinear surface waves in the small-amplitude approximation, deriving the wave packet envelope equation as a nonlinear Schrödinger equation (NLS). In later studies, more complex forms were obtained: a higher-order NLS with fifth-order nonlinearity for wave envelopes on the surface of a finite-depth fluid was derived in [3]; the six-wave interaction and classical three-wave equations were derived from the free surface gravity wave equation with surface tension in [4].

Additionally, it is essential to highlight articles [5] and [6] that focus on analytical studies addressing the impact of surface tension in problems related to wave propagation on free surfaces and fluid interfaces.

Below we present some studies on the propagation of nonlinear waves in layer fluids analysed in the setting of multiple-scale expansions. Hasimoto and Ono [7] used a multiple-scale expansion to express a weakly nonlinear solution in the form of a modulated wave packet that propagates on a water layer, whose envelope evolves according to the NLS. In the article [8], a study on the propagation of wave packets along the interface of two fluid half-spaces with surface tension is presented, and evolution equation of the envelope was derived in the form of NLS. The stability of finite--amplitude interfacial progressive waves in a two-layer fluid to small perturbations is discussed by Grimshaw and Pullin [9], and NLS is obtained to describe slowly modulated waves using a multiscale expansion. The nonlinear problem of wave-packet propagation along the interface of two semi-infinite fluids is studied via a fourth--order multiple scale method by Selezov et al. [10]. We also mention several articles in which the multi-scale expansion method was used to investigate nonlinear wave motions in two-component hydrodynamic media in the presence of flows [11–15]. Note that the method of multiple-scale expansions requires complex transformations, making it challenging to apply as the complexity of the model under study increases, but modern computer algebra systems help overcome the complexity that was the argument for choosing this method for this study.

The following studies explore the role of the Benjamin-Feir instability in hydrodynamic environments, with emphasis on stabilization by dissipation and its influence on extreme wave formation. In [16], it is shown that for waves with narrow bandwidth and moderate amplitude, specific dissipation stabilizes the instability, as confirmed by experiments. Direct simulations in [17] support these findings, indicating the importance of dissipation models. Onorato et al. [18] demonstrate that the Benjamin-Feir index correlates with modulational instability and extreme wave probability, while [19] and [20] discuss nonlinear processes and dispersive shock waves arising from modulation instability. Zakharov and Ostrovsky [19] explore nonlinear processes from modulation instability, while El and Hoefer [20] survey dispersive hydrodynamics, focusing on dispersive shock waves. In [21], wind-viscosity balance regimes for wave propagation are identified and validated experimentally. Spectral methods in [22,23] provide new insights into eigenvalues of the Benjamin-Feir instability, detailing stability characteristics near the Stokes wave.

As can be seen from the above, despite the great interest in the phenomenon of modulation stability, there is currently no comprehensive study of it in relation to internal wave packets on the contact surface that takes surface tension into account. This article presents investigations of modulational stability in a layered hydrodynamic system ‘half-space – layer with a rigid lid’ (HS-La) taking into account the surface tension by multiscale analysis performed by symbolic computations. The reliability of the obtained results is confirmed by the limiting cases of infinitely increasing layer thickness for transitions to the system ‘half-space – half-space’ (HS-HS).

2. Problem statement and research method

The problem of wave packet propagation along the contact surface $z = \eta(x,t)$ of two liquid incompressible media Ω_1 and Ω_2 is investigated. The densities of the layers are denoted as ρ_1 and ρ_2, respectively. The analysis includes the surface tension force T acting on the contact surface of the liquid media. The gravitational force is directed perpendicular to the contact surface in the negative direction.

Figure 1 illustrates a graphical representation for the HS-La model. The regions in the system in an undisturbed state have the following form: $\Omega_1 = \{(x,z)| -\infty < x < +\infty, -\infty < z < 0\}$ and $\Omega_2 = \{(x,z)| -\infty < x < +\infty, 0 < z < h_2\}$.

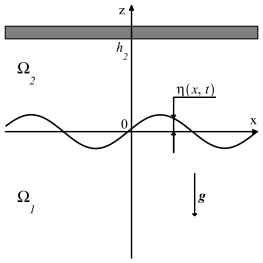

Fig. 1. Statement of the problem

The mathematical formulation of the problem for investigating the HS-La model will be presented in dimensionless form. Let's take the following parameters as the basis for dimensionless quantities: the acceleration due to gravity g, the density of the lower fluid ρ_1, and the characteristic surface tension T_0. Then, the characteristic length is $L = \left(T_0\rho_1^{-1}g^{-1}\right)^{1/2}$, the characteristic time is $t_0 = \left(Lg^{-1}\right)^{1/2}$, and the characteristic mass is $m_0 = \rho_1 L^3$. Let's introduce a small dimensionless parameter characterizing the steepness of the wave $\alpha = a/l$, where a is the maximum elevation of the contact surface $\eta(x,t)$, and l is the wavelength. Based on the characteristic quantities and small parameter, dimensionless quantities denoted with asterisks are introduced in the form

$$L(x^*, z^*, h_2^*) = (x, z, h_2),\ t_0 t^* = t,\ T_0 T^* = T,\ \alpha L \eta^* = \eta,\ \alpha L^2 t_0^{-1}(\phi_1^*, \phi_2^*) = (\phi_1, \phi_2) \tag{1}$$

It is necessary to provide an explanation regarding the features and advantages of introducing dimensionless quantities in the form of (1) compared to those proposed by Nayfeh [8], as stability diagrams for various geometric and physical characteristics of the considered HS-La system, along with their comparison to the stability diagram obtained by Nayfeh for the system HS-HS, will be presented in Section 3. Nayfeh non-dimensionalizes the problem using the actual surface tension, where the actual surface tension appears in the characteristic length $(T\rho_1^{-1}g^{-1})^{1/2}$ and in the characteristic time $(lg^{-1})^{1/2}$, resulting in his non-dimensional formulation containing only one dimensionless parameter, $\rho = \rho_2/\rho_1$, since he subsequently introduces $\varepsilon \ll 1$ to characterize wave amplitude. As a result of this non-dimensionalization, the dimen-

sionless surface tension coefficient effectively becomes 1, and all of Nayfeh's calculations correspond to this assumption. This approach does not allow for the exploration of the effect of varying surface tension at the interface of the liquid half-spaces. In our case, by using the non-dimensionalization formulae (1), the characteristic value of the surface tension coefficient T_0 is fixed, allowing us to vary the dimensionless value of the coefficient. In Subsection 3.2, the influence of geometric parameters on the modulational stability of the HS-La system at characteristic surface tension, i.e., for $T^* = 1$, is studied, and in Subsection 3.3, the results are presented for surface tension values $T^* \neq 1$ differing from the characteristic value.

The propagation velocities of the packets in the regions Ω_j are expressed through the gradients of potentials $\phi_j(x,z,t)$ $(j = 1,2)$, and the mathematical statement of the problem of wave packet propagation in the HS-La model is in the form

$$\begin{gathered}
\Delta\phi_j = 0 \quad \text{in} \quad \Omega_j, \\
\eta_{,t} - \phi_{j,z} = -\alpha\eta_{,x}\phi_{j,x} \quad \text{at} \quad z = \alpha\eta(x,t), \\
\phi_{1,t} - \rho\phi_{2,t} + (1-\rho)\eta + 0.5\alpha\left(\nabla\phi_1\right)^2 - 0.5\alpha\rho\left(\nabla\phi_2\right)^2 \\
-T\left(1+(\alpha\eta_{,x})^2\right)^{-1.5}\eta_{,xx} = 0 \quad \text{at} \quad z = \alpha\eta(x,t)
\end{gathered} \tag{2}$$

with boundary conditions at the depth $z \to -\infty$ and on the rigid lid $z = h_2$

$$|\nabla\phi_1| \to 0 \quad \text{at} \quad z \to -\infty, \quad \phi_{2,z} = 0 \quad \text{at} \quad z = h_2. \tag{3}$$

Following the method of multi-scale expansions, let's represent the sought surface elevation and velocity potentials in the domains $\Omega_j (j = 1,2)$ as follows

$$\begin{aligned}
\eta(x,t) &= \sum_{n=1}^{3}\alpha^{n-1}\eta_n(x_0,x_1,x_2,t_0,t_1,t_2) + \mathrm{O}(\alpha^3), \\
\phi_j(x,z,t) &= \sum_{n=1}^{3}\alpha^{n-1}\phi_{jn}(x_0,x_1,x_2,z,t_0,t_1,t_2) + \mathrm{O}(\alpha^3),
\end{aligned} \tag{4}$$

where $x_n = \alpha^n x$, $t_n = \alpha^n t$ are the spatial and temporal scaling variables.

The substitution (4) into the problem (2)-(3) leads to the first three linear approximations with respect to the unknown functions, which are coefficients in the expansion (4). Here are the solutions for the first approximation

$$\eta_1(x,t) = A\exp(\mathrm{i}\theta) + \overline{A}\exp(-\mathrm{i}\theta), \tag{5}$$

$$\phi_{11}(x,z,t) = -\frac{\mathrm{i}\omega}{k}\left(A\exp(\mathrm{i}\theta + kz) - \overline{A}\exp(-\mathrm{i}\theta + kz)\right), \tag{6}$$

$$\phi_{21}(x,z,t) = \frac{\mathrm{i}\omega}{k\sinh(kh_2)}\left(A\exp(\mathrm{i}\theta) - \overline{A}\exp(-\mathrm{i}\theta)\right)\cosh(k(h_2 - z)), \tag{7}$$

where $A = A(x_1,x_2,t_1,t_2)$ is the envelope of the wave packet, $\overline{A}$ is the complex conjugate of A, k is the wave number, ω is the frequency of the wave packet center, $\theta = kx_0 - \omega t_0$. The dispersion relation is given by

$$\omega^2 = \frac{k - \rho k + Tk^3}{1 + \rho \coth(kh_2)}. \tag{8}$$

Based on these solutions of the first approximation (5)-(7) and the dispersion relation (8), conditions of solvability and solutions of the second approximation are obtained. Below is the analytical expression for $\eta_2(x,t)$

$$\eta_2(x,t) = b_0 A\overline{A} + \Lambda A^2 \exp(2\mathrm{i}\theta) + \text{c.c.} \tag{9}$$

where c.c. denotes the complex conjugate of the preceding expression and

$$b_0 = \frac{\rho\omega^2}{2(1-\rho)\sinh^2(kh_2)},\ \Lambda = \frac{k\omega^2\coth(kh_2)\left(2\sinh^2(kh_2)(1-\rho)-3\rho\right)}{2\cosh(2kh_2)\omega^2\rho - (4Tk^3+k-k\rho-2\omega^2)\sinh(2kh_2)}.$$

The solvability condition for the second approximation is in the form

$$W_{11}A_{,t_1} + W_{12}A_{,x_1} = 0, \tag{10}$$

where the coefficients W_{11} and W_{12} depend only on T, ρ, k, and h_2. Here and throughout the text, the partial derivatives of the envelope A with respect to the corresponding variables are introduced in this form $A_{,t_1} = \partial A/\partial t_1$, $A_{,x_1} = \partial A/\partial x_1$ and others. After transformations, the condition (10) can be rewritten as

$$A_{,t_1} + \omega' A_{,x_1} = 0, \tag{11}$$

where $\omega' = \partial\omega/\partial k$ is the group velocity.

For the problem of the third approximation, the solvability condition is in the form

$$W_{21}A_{,t_2} + W_{22}A_{,x_2} + W_{23}A_{,x_1x_1} + W_{24}A^2\overline{A} = 0, \tag{12}$$

where the coefficients W_{21}, W_{22}, W_{23}, and W_{24} depend only on T, ρ, k, h_2. After analytical transformations, considering the dispersion relation (8), equations (11) and (12), and transitioning from the scaling variables $t_0, t_1, t_2, x_0, x_1, x_2$ to variables x and t, the evolution equation can be written as

$$\mathrm{i}A_{,t} + \mathrm{i}\omega' A_{,x} + 0.5\omega'' A_{,xx} = -\alpha\omega^{-1} J A^2\overline{A}, \tag{13}$$

where $\omega'' = \partial^2\omega/\partial k^2$, J is a coefficient depending only on T, ρ, k, h_2. The form of the coefficient J, the Benjamin-Feir index, is quite cumbersome and is presented in the Appendix. Transitioning to a moving frame with the group velocity by substituting $\xi = x - \omega' t$ and $\zeta = t$, let's rewrite the envelope equation (13) in the form of an NLS

$$\mathrm{i}A_{,\zeta} + 0.5\omega'' A_{,\xi\xi} = -\alpha\omega^{-1} J A^2\overline{A}. \tag{14}$$

To derive the modulation stability condition of wave packets, let's consider one of the solutions of the equation (14) which depends only on time

$$A = a\exp(\mathrm{i}\alpha a^2\omega^{-1}J\zeta), \tag{15}$$

where a is a constant. Substituting (15) into (5) and (9), taking into account the expansion (4), and transitioning from variables (ξ,ζ) to (x,t), we obtain

$$\eta(x,t) = 2a\cos(kx-\hat{\omega}t) + 2\alpha a^2\left(b_0+\Lambda\cos(2kx-2\hat{\omega}t)\right) + \mathrm{O}(\alpha^2), \tag{16}$$

where $\hat{\omega} = \omega - \alpha a^2\omega^{-1}J$. Utilizing the methodology described in [8], based on (14), (15), and (16), we obtain the modulation or Benjamin-Feir stability condition for wave packets in the HS-La model in the form of

$$J\omega'' < 0. \tag{17}$$

It's worth noting that condition (17) coincides with the condition obtained for the HS-HS model of wave propagation at the interface between two semi-infinite regions, as described in [8]. It is important to note that the limiting transition from the HS-La system to the HS-HS system occurs as $h_2 \to +\infty$, during which the dispersion equation, solvability conditions, and the evolution equation, as well as the expressions for Λ and J, degenerate into the corresponding equations and expressions previously derived in [8] for the HS-HS system that confirms the correctness of the results.

3. Stability analysis depending on the parameters of the hydrodynamic system

3.1. Notations on the stability diagrams

In this section, a description and analysis of stability diagrams on the (ρ,k) plane for the HS-La system are presented. Each stability diagram is divided into regions of linear instability (dark shading) and linear stability. The region of linear stability, in turn, consists of areas of nonlinear stability (unshaded) and nonlinear instability, or in other words – instability of the envelope of the wave packet, or modulational instability, or Benjamin-Feir instability (light shading). The condition for linear stability is determined when the wave numbers are greater than a critical value $k_c=\sqrt{(\rho-1)/T}$, therefore, in all the stability diagrams presented below, the (ρ,k) plane is divided by the curve $k = k_c$ (black curve) into a region of linear instability located below this curve, and a region of linear stability located above and to the left of it.

As previously indicated in (17), the sign of the expression $J\omega''$ determines whether the envelope of the wave packet is stable or not, i.e., whether modulational stability exists or not. Thus, the region of linear stability is divided into regions of nonlinear stability and instability by curves along which $J = 0$ (red curves), $J \to \infty$ (blue curves), and $\omega'' = 0$ (green curves). Below is a description of the regions of modulational stability and instability, which will be referred to as 'stability' and 'instability' regions for brevity in the following discussion.

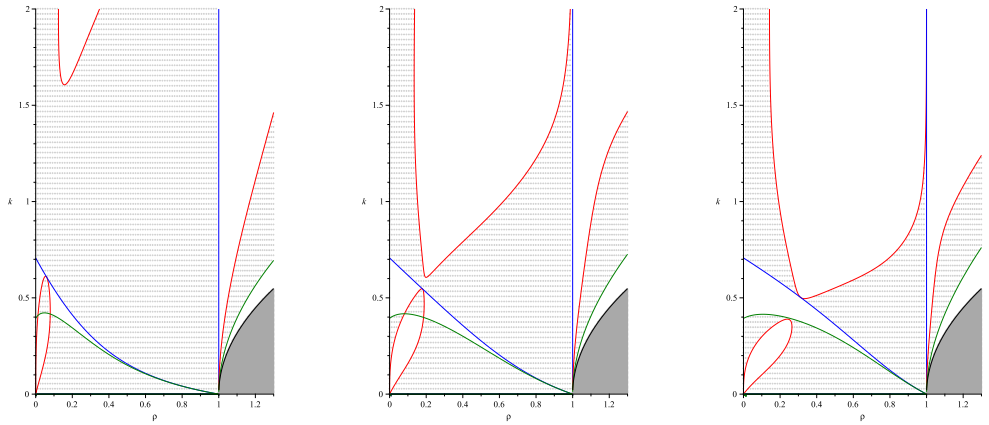

a) $h_2 = 0.5$ b) $h_2 = 1$ c) $h_2 = 1.5$

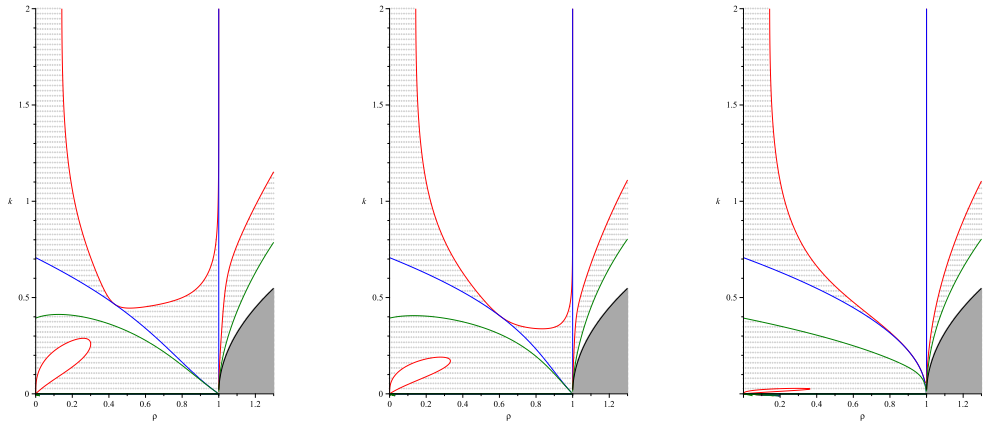

d) $h_2 = 2$ e) $h_2 = 3$ f) $h_2 = 20$

Fig. 2. Modulational stability diagram of wave packets in HS-La system for $T = 1$

3.2. Modulational stability dependence on geometrical parameters

The stability diagrams for the HS-La system are presented in Figure 2.

To begin with, we note the existence of a rather extensive region of modulational stability at large wave numbers, i.e., in the realm of capillary waves. We shall denote this region as the 'upper' region. For small values of layer thickness, the 'upper' region is situated relatively high: for $h_2 = 0.5$, the lower boundary of this region lies approximately at $\rho \simeq 0.16$, $k \simeq 1.61$ (Fig. 2a), while for $h_2 = 1$, the lower boundary is significantly lower, at $\rho \simeq 0.21$, $k \simeq 0.59$ (Fig. 2b). With an increase in layer thickness, the lower boundary of the 'upper' stability region approaches closely to the blue curve along which $J \to \infty$. It is evident that for thicknesses $h_2 = 1.5,\ 2,\ 3$ (Figs 2c, d, e), the 'upper' region almost touches the curve delineating another stability region from above, which we shall term as 'elongated'. With a substantial increase in layer thickness to $h_2 = 20$ (Fig. 2f), the lower boundary of the 'upper' region of nonlinear

stability tends towards the point $\rho = 1$, $k = 0$. This behavior is in good agreement with the asymptotic degeneration of the HS-La system into the HS-HS system as $h_2 \to \infty$ [8]. Concluding the description of the 'upper' region, it is noteworthy that irrespective of the layer thickness, this region exhibits two vertical asymptotes at $\rho = 1$ and $\rho \simeq 0.1716$. In Figure 3, the behavior in the vicinity of the asymptote $\rho \simeq 0.1716$ of the boundary between the region of instability and the 'upper' stability region is presented for values of $h_2 = 0.5, 0.75, 1, 1.5, 20$. It can be observed that the boundary of these regions shifts to the left as the layer thickness decreases. As expected, with increasing layer thickness, the curve degenerates into the previously known case as $h_2 \to \infty$ [8], which is clearly visible for $h_2 = 20$.

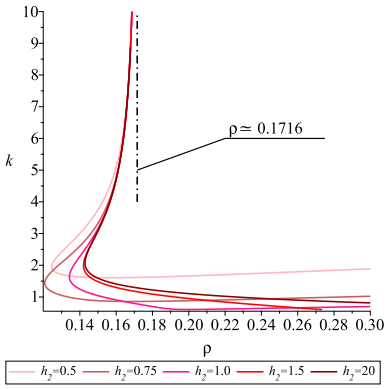

Fig. 3. The vicinity of the asymptote in HS-La system for $T = 1$

We turn now to other regions of the HS-La system diagram for long waves with $k < 0.7$. The first is the 'elongated' region, bounded above by the blue curve where $J \to \infty$, and below by the green curve where $\omega'' = 0$. The second region is a 'loop' emerging from the origin, bounded by the red curve where $J = 0$. For small upper layer thicknesses ($h_2 = 0.5,\ 1.0$), the 'elongated' region and 'loop' intersect, creating a complex pattern of stability and instability at low density ratios (see Figs 2a, b). With larger thicknesses, however, the 'elongated' region and 'loop' remain separate as shown for $h_2 = 1.5, 2, 3, 20$ in Figures 2c, d, e, f.

Below, we note some properties of the 'elongated' region and the 'loop'. With increasing layer thickness, the 'elongated' region widens, and for $h_2 = 20$ (Fig. 2f), it almost coincides with a similar region in the case of two half-spaces [8]. This region terminates at $\rho = 1$ and $k = 0$. If we set $\rho = 0$, i.e., in the case of degeneration of this system into a liquid half-space, then the 'elongated' region corresponds to the interval of wavenumbers $k \in (0.393,\ 0.707)$ for all thicknesses of the upper layer. This result was previously obtained in the study of nonlinear stability of waves on the free surface of a liquid half-space [2] and was also confirmed in [8].

For small layer thicknesses, the 'loop' is almost vertically oriented, as depicted for $h_2 = 0.5$ (Fig. 2a). As the layer thickness increases, the 'loop' rotates clockwise around the origin (see Figs 2b, c, d, e), and for sufficiently large thicknesses, it practically aligns with the horizontal axis, as clearly seen for $h_2 = 20$ in Figure 2f. It is

evident that upon degeneration of the HS-La system, the 'loop' completely vanishes, merging with the horizontal axis, consistent with [8].

As evident from Figure 2, the diagram is divided by the vertical line $\rho = 1$ into two parts: the region of nonlinear instability narrowing upwards on the left, and the region of stability on the right. As noted earlier, with increasing layer thickness, the 'upper' stability region descends and progressively approaches the asymptote $\rho = 1$. However, for each finite value of thickness, there exists a narrow region of instability separating the stability regions to the right and left of $\rho = 1$, along which $J \to \infty$. Upon degeneration of the considered system into two half-spaces, the stability regions merge into a single large region of nonlinear stability [8].

In conclusion of the description of the stability diagram for the HS-La system, let us address the region of $\rho > 1$ physically improbable in hydrodynamics. This result may be valuable in other scientific domains where similar weakly nonlinear mathematical models are permissible. In the right part of the diagram, beyond $\rho = 1$, all curves delineating regions in this part of the diagram emanate from the point $(1,0)$, with stability and instability regions alternating. As previously mentioned, the region of nonlinear stability lies above all others. It is bounded from below by the red curve. Below this curve lies the region of nonlinear instability, bounded from below by the green curve. Further below lies the region of nonlinear stability, which borders the region of linear instability along the black curve $k = k_c$.

3.3. Modulational stability dependence on surface tension

In Figures 4a-c, stability diagrams for the HS-La system are presented for a layer thickness of $h_2 = 1$ and surface tension coefficient values of $T = 0.75,\ 1.25,\ 1.75$. It can be observed that an increase in surface tension at the interface between liquid media significantly distorts the stability diagram. This is particularly evident in the behavior of the 'elongated' stability region, which becomes substantially wider, shifting towards the long-wave regime for all density values, including $\rho = 0$, corresponding to surface waves. The 'elongated' region and the 'loop' noticeably decrease with increasing surface tension, while the 'upper' stability region becomes more separated from them by a considerable area of instability.

It should be noted that at these parameter values, the qualitative pattern on the stability diagram remains unchanged. However, in the case of the HS-La system with $h_2 = 1.5$ with $T = 0.75, 1.25, 1.75$ (Figs 4d, e, f), not only is the deformation of the diagram observed but also qualitative changes. As noted earlier, at a fixed layer thickness of $h_2 = 1.5$ and $T = 1$, the 'elongated' region and the 'loop' do not intersect (Fig. 2c), thereby forming two regions of nonlinear stability. With a decrease in the surface tension coefficient to $T = 0.75$, a similar pattern emerges. Additionally, with an increase in the surface tension coefficient to $T = 1.25, 1.75$ the 'loop' intersects with the 'elongated' region, and the configuration of regions qualitatively resembles the pattern for $h_2 = 1$ and $T = 0.5$. In this case, the lower boundary of the 'upper' region shifts downward, approaching close to the uppermost point of the 'loop'.

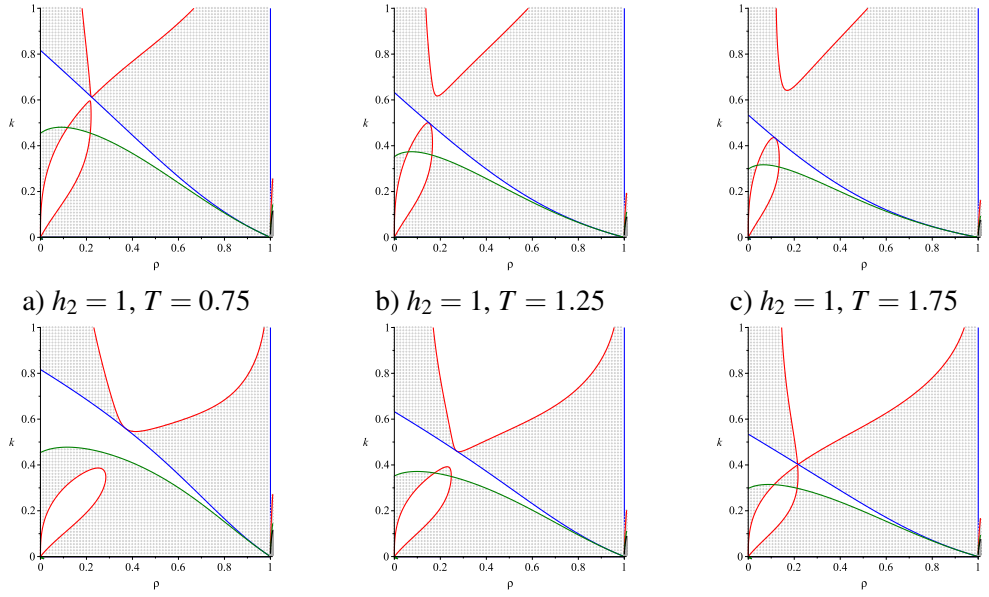

a) $h_2 = 1$, $T = 0.75$ b) $h_2 = 1$, $T = 1.25$ c) $h_2 = 1$, $T = 1.75$

d) $h_2 = 1.5$, $T = 0.75$ e) $h_2 = 1.5$, $T = 1.25$ f) $h_2 = 1.5$, $T = 1.75$

Fig. 4. Modulational stability diagram of wave packets in the HS-La system

4. Conclusions

Let us summarize the main characteristics of the regions of modulational stability in the two-dimensional hydrodynamic HS-La system on the $(\rho,\ k)$ plane for various values of layer thickness and surface tension. For $\rho < 1$, three characteristic stability regions have been identified: the 'upper', 'elongated', and 'loop' regions.

For small layer thicknesses: (i) the 'upper' region is located in the high wavenumber region, covering a significant range of density ratios, with asymptotes at $\rho \simeq 0.1716$ and $\rho = 1$; (ii) for $k < 0.7$, two regions exist, the 'elongated' and 'loop', which for some layer thickness values do not intersect, while for others they do, forming a complex configuration of stability and instability regions; (iii) parameters of the system have been identified – layer thickness and surface tension – where the 'loop' and 'elongated' regions intersect, with the boundary of the 'loop' critically approaching the boundary of the 'upper' region. For large layer thicknesses: (i) stability regions do not intersect; (ii) the 'upper' region covers a wide range of wavenumbers, including relatively small ones; (iii) the 'elongated' region significantly expands; (iv) the 'loop' is located in the region of gravity waves.

This research lays the groundwork for further analysis of wave packet propagation in two-layer systems such as "layer-half-space" and "layer-layer", where modulational stability regions may shift or newly emerge, especially at small wave numbers.

Acknowledgement

Dr. Olga Avramenko expresses gratitude to the Research Council of Lithuania for the support in preparing this article.

References

[1] Benjamin, T.B., & Feir, J.E. (1967). The disintegration of wave trains on deep water Part 1. Theory. *J. Fluid Mech.*, *27*(3), 417-430, DOI: 10.1017/S002211206700045X.

[2] Zakharov, V.E. (1968). Stability of periodic waves of finite amplitude on the surface of a deep fluid. *J. App. Mech. Techn. Phys.*, *9*, 190-194, DOI: 10.1007/BF00913182.

[3] Sedletsky, Y. (2021). A fifth-order nonlinear Schrödinger equation for waves on the surface of finite-depth fluid. *Ukr. J. Phys.*, *66*(1), 41-54, DOI: 10.15407/UJPE66.1.41.

[4] Ablowitz, M.J., Luo, H.-D., & Musslimani, Z.H. (2023). Six wave interaction equations in finite-depth gravity waves with surface tension. *J. Fluid Mech.*, *961*, A3, DOI: 10.1017/jfm .2023.128.

[5] Ionescu, A.D., & Pusateri, F. (2018). Global regularity for 2D water waves with surface tension. *Mem. Amer. Math. Soc.*, *256*, 123 pp., DOI: 10.48550/arXiv.1408.4428.

[6] Düll, W.P. (2021). Validity of the nonlinear Schrödinger approximation for the two-dimensional water wave problem with and without surface tension in the arc length formulation. *Arch. Rational Mech. Anal.*, *239*, 831-914, DOI: 10.1007/s00205-020-01586-4.

[7] Hasimoto, H., & Ono, H. (1972). Nonlinear modulation of gravity waves. *J. Phys. Soc. Japan*, *33*(3), 805-811, DOI: 10.1143/JPSJ.33.805.

[8] Nayfeh, A. (1976). Nonlinear propagation of wave-packets on fluid interface. *Trans. ASME, Ser. E: J. Appl. Mech.*, *43*(4), 584-588, DOI: 10.1115/1.3423936.

[9] Grimshaw, R.H.J., & Pullin, D.I. (1985). Stability of finite-amplitude interfacial waves. Part 1. Modulational instability for small-amplitude waves. *J. Fluid Mech.*, *160*, 297-315, DOI: 10.10 17/S0022112085003494.

[10] Selezov, I., Avramenko, O., Kharif, C., & Trulsen, K. (2003). High-order evolution equation for nonlinear wave-packet propagation with surface tension accounting. *Comptes Rendus. Mécanique*, *331*(3), 197-201, DOI: 10.1016/S1631-0721(03)00043-3.

[11] Abrashkin, A.A., & Pelinovsky, E.N. (2018). Dynamics of a wave packet on the surface of an inhomogeneously vortical fluid (Lagrangian description). *Izv. Atmos. Ocean. Phys.*, *54*, 101-105, DOI: 10.1134/S0001433818010036.

[12] Li, S., Chen, J., Cao, A., & Song, J. (2019). A nonlinear Schrödinger equation for gravity waves slowly modulated by linear shear flow. *Chinese Phys. B*, *28*, 124701, DOI: 10.1088/1674-1056/ ab53cf.

[13] Li, S., Xie, X., Chen, D., & Song, J. (2022). Modulation effect of linear shear flow on interfacial waves in a two-layer fluid with finite layer depths. *Phys. Fluids*, *34*, 092105, DOI: 10.1063/ 5.0098077.

[14] Pal, T., & Dhar, A.K. (2022). Stability analysis of finite amplitude interfacial waves in a two- -layer fluid in the presence of depth uniform current. *Ocean Dynam.*, *72*, 241-257, DOI: 10.1007/s10236-022-01503-1.

[15] Pal, T., & Dhar, A.K. (2024). Weakly nonlinear modulation of interfacial gravity-capillary waves. *Ocean Dynam.*, *74*, 133-147, DOI: 10.1007/s10236-023-01594-4.

[16] Segur, H., Henderson, D., Carter, J., Hammack, J., Li, C., Pheiff, D., & Socha, K. (2005). Stabilizing the Benjamin-Feir instability. *J. Fluid Mech.*, *539*, 229-271, DOI: 10.1017/S002211 200500563X.

[17] Wu, G., Liu, Y., & Yue, D.K.P. (2006). A note on stabilizing the Benjamin-Feir instability. *J. Fluid Mech.*, *556*, 45-54, DOI: 10.1017/S0022112005008293.

[18] Onorato, M., Osborne, A.R., Serio, M., Cavaleri, L., Brandini, C., & Stansberg, C.T. (2006). Extreme waves, modulational instability and second order theory: wave flume experiments on irregular waves. *Europ. J. Mech. – B/Fluids*, *25*(5), 586-601, DOI: 10.1016/j.euromechflu.2006.01.002.

[19] Zakharov, V.E., & Ostrovsky, L.A. (2009). Modulation instability: The beginning. *Physica D: Nonlinear Phenom.*, *238*(5), 540-548, DOI: 10.1016/j.physd.2008.12.002.

[20] El, G.A., & Hoefer, M.A. (2016). Dispersive shock waves and modulation theory. *Physica D: Nonlinear Phenom.*, *333*, 11-65, DOI: 10.1016/j.physd.2016.04.006.

[21] Armaroli, A., Eeltink, D., Brunetti, M., & Kasparian, J. (2018). Nonlinear stage of Benjamin-Feir instability in forced/damped deep-water waves. *Phys. Fluids*, *30*(1), 017102, DOI: 10.1063/1.5006139.

[22] Berti, M., Maspero, A., & Ventura, P. (2022). Full description of Benjamin-Feir instability of Stokes waves in deep water. *Invent. Math.*, *230*, 651-711, DOI: 10.1007/s00222-022-01130-z.

[23] Berti, M., Maspero, A., & Ventura, P. (2023). Benjamin-Feir instability of Stokes waves in finite depth. *Arch. Rat. Mech. Anal.*, *247*, 91, DOI: 10.1007/s00205-023-01916-2.

Appendix

The expression for J from (17) in HS-La model

$$J = \frac{W_1\omega^6 + W_2\omega^4 + W_3\omega^2 + W_4}{W_5\omega^2 + W_6}k,$$

where $W_1 = \rho^3\cosh(2kh_2)\mathrm{csch}^3(kh_2) + 2\rho^2\mathrm{csch}(kh_2)\coth(kh_2),$

$$\begin{aligned}
W_2 = {} & -6k\sinh^2(kh_2)\cosh(kh_2) + 2k\rho\big[\cosh(2kh_2)\mathrm{csch}(kh_2) \\
& + 2\cosh(2kh_2)\cosh(kh_2) - 6\sinh(kh_2)\cosh^2(kh_2) + \cosh^3(kh_2) \\
& + \cosh(2kh_2)\cosh(kh_2)\coth(kh_2)\big] - k\rho^2\big[2\cosh(2kh_2)\mathrm{csch}(kh_2) \\
& + 6\cosh(2kh_2)\cosh(kh_2) + 1.5\coth(kh_2)\mathrm{csch}(kh_2) \\
& - 2\sinh^2(kh_2)\cosh(kh_2) + 2\cosh(2kh_2)\coth(kh_2)\mathrm{csch}(kh_2) \\
& - 12\sinh(kh_2)\cosh^2(kh_2) + 2\cosh(2kh_2)\cosh(kh_2)\coth(kh_2)\big] \\
& + k\rho^3\big[5.5\coth(kh_2)\mathrm{csch}(kh_2) + 2\cosh(2kh_2)\cosh(kh_2)\coth^2(kh_2) \\
& - 6\cosh^2(kh_2)\coth(kh_2)\mathrm{csch}(kh_2) + 2\coth(kh_2)\mathrm{csch}(kh_2)\cosh^4(kh_2)\big] \\
& - 4Tk^3\rho^2\mathrm{csch}(kh_2)\coth(kh_2),
\end{aligned}$$

$$\begin{aligned}
W_3 = {} & k^2(1-\rho)\big[(1-\rho)\{2\cosh(kh_2)\sinh^2(kh_2) \\
& + 6\sinh(kh_2)\cosh^2(kh_2) - 2\rho\cosh(kh_2)\cosh(2kh_2)\coth(kh_2)\} \\
& - 1.5Tk^2\rho\cosh(2kh_2)\mathrm{csch}(kh_2) + 11Tk^2\cosh(kh_2)\sinh^2(kh_2) \\
& + 24Tk^2\rho\cosh^2(kh_2)\sinh(kh_2) - 6.5Tk^2\rho\cosh(kh_2)\cosh^2(kh_2)\mathrm{csch}(kh_2)\big],
\end{aligned}$$

$$W_4 = Tk^5\big(1-\rho\big)\big[1.5\rho - 1.5 - 6Tk^2\big]\cosh(kh_2)\sinh^2(kh_2),$$
$$W_5 = 2\big(1-\rho\big)\big(\sinh(kh_2)+\rho\cosh(kh_2)\big)\big(\sinh(2kh_2)+\rho\cosh(2kh_2)\big),$$
$$W_6 = k\big(1-\rho\big)\big(1-\rho+4Tk^2\big)\big(\sinh(kh_2)-\rho\cosh(kh_2)\big)\sinh(2kh_2).$$